ACADEMIC PRESS

Available online at www.sciencedirect.com

SCIENCE DIRECT®

DEVELOPMENTAL BIOLOGY

Developmental Biology 261 (2003) 381–390

www.elsevier.com/locate/ydbio

Calcium transients triggered by planar signals induce the expression of *ZIC3* gene during neural induction in *Xenopus*

Catherine Leclerc,[a] Michelle Lee,[b] Sarah E. Webb,[b] Marc Moreau,[a,*] and Andrew L. Miller[b]

[a] *Centre de Biologie du Développement, UMR 5547, Université Paul Sabatier, 118 Route de Narbonne, F-31062 Toulouse, CEDEX 04, France*
[b] *Department of Biology, The Hong Kong University of Science and Technology, Clear Water Bay, Kowloon, Hong Kong, PRC*

Received for publication 24 January 2003, revised 25 April 2003, accepted 28 April 2003

Abstract

In intact *Xenopus* embryos, an increase in intracellular Ca^{2+} in the dorsal ectoderm is both necessary and sufficient to commit the ectoderm to a neural fate. However, the relationship between this Ca^{2+} increase and the expression of early neural genes is as yet unknown. In intact embryos, studying the interaction between Ca^{2+} signaling and gene expression during neural induction is complicated by the fact that the dorsal ectoderm receives both planar and vertical signals from the mesoderm. The experimental system may be simplified by using Keller open-face explants where vertical signals are eliminated, thus allowing the interaction between planar signals, Ca^{2+} transients, and neural induction to be explored. We have imaged Ca^{2+} dynamics during neural induction in open-face explants by using aequorin. Planar signals generated by the mesoderm induced localized Ca^{2+} transients in groups of cells in the ectoderm. These transients resulted from the activation of L-type Ca^{2+} channels. The accumulated Ca^{2+} pattern correlated with the expression of the early neural precursor gene, *Zic3*. When the transients were blocked with pharmacological agents, the level of *Zic3* expression was dramatically reduced. These data indicate that, in open-face explants, planar signals reproduce Ca^{2+} -signaling patterns similar to those observed in the dorsal ectoderm of intact embryos and that the accumulated effect of the localized Ca^{2+} transients over time may play a role in controlling the expression pattern of *Zic3*.

Keywords: Neural determination; Planar signals; Calcium signalling; Calcium imaging; Aequorin; Zic3

Introduction

Neural induction in vertebrates occurs during gastrulation when the dorsal ectodermal cells become committed to form neurectoderm and follow a neural rather than epidermal fate (reviewed by Hamburger, 1988). In amphibian embryos, neural induction is generally regarded as being a default pathway, as it only occurs when the potent epidermal inducer Bone Morphogenetic Protein-4 (BMP4; Hawley et al., 1995; Zimmerman et al., 1996; reviewed by Sasai and De Robertis, 1997) is inactive. BMP4 is expressed throughout the animal hemisphere; however, in the dorsal ectoderm it forms high affinity complexes with noggin, chordin, and follistatin, which are secreted by Spemann's Organizer (Lamb et al., 1993; Hemmati-Brivanlou et al., 1994; Sasai et al., 1995). In this state, BMP4 cannot induce the ectodermal cells to form epidermis and so instead they become committed to a neural fate. However, we have previously shown in *Pleurodeles waltl* embryos that an increase in intracellular Ca^{2+} in the dorsal ectoderm is both necessary and sufficient to commit the ectoderm to a neural fate (Moreau et al., 1994; Leclerc et al., 1995, 1997). In addition, we recently reported that, by loading intact *Xenopus* embryos with aequorin, a Ca^{2+} -sensitive bioluminescent protein, and using a Photon Imaging Microscope (PIM), distinct patterns of Ca^{2+} signaling can be visualized during the gastrulation period (Leclerc et al., 2000). Localized transient domains of elevated Ca^{2+} were observed exclusively in the anterior dorsal part of the ectoderm, and these transients increased in number and

* Corresponding author. Fax: +33-5-61-55-65-07.
E-mail address: moreau@cict.fr (M. Moreau).

0012-1606/03/$ – see front matter © 2003 Elsevier Inc. All rights reserved.
doi:10.1016/S0012-1606(03)00298-7

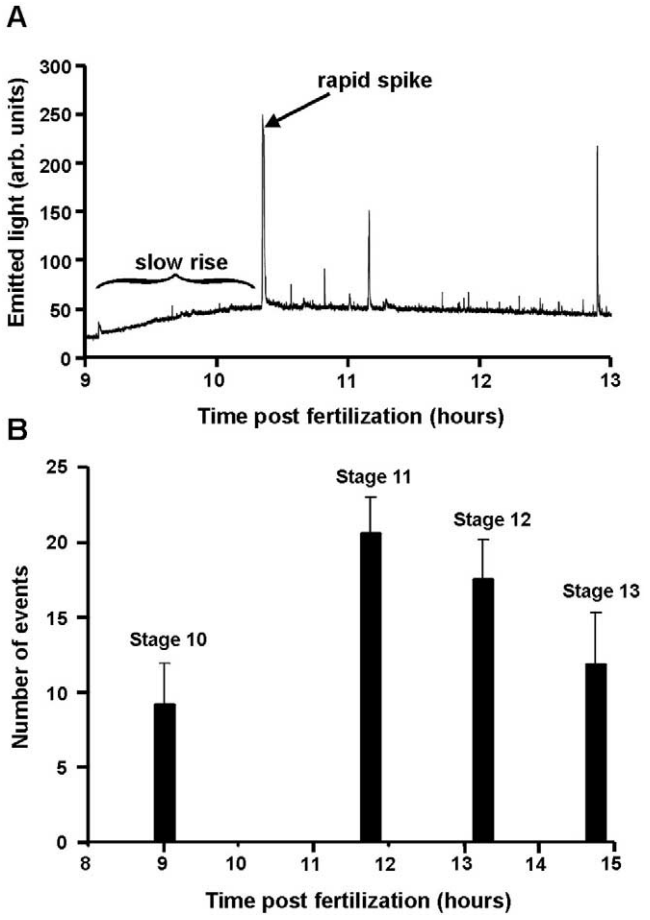

Fig. 1. The changes in intracellular Ca^{2+} that occur in explants during gastrulation. (A) A representative example of a PMT trace obtained from an aequorin-loaded explant. Data collection was started at 9 hpf (stage 10) when the explant was prepared, and was ended at 13 hpf (stage 12). Two components are visible on the trace: a slow-rising component and rapid spikes. Emitted light is expressed in arbitrary (arb.) units. (B) The average number of Ca^{2+} transients observed from explants. The maximum number of events occurs at stage 11. Mean ± SEM of five explants is shown.

amplitude between stages 9 and 11, i.e., they occurred at the right time and in the right place to correlate with neural induction (Leclerc et al., 2000). No increase in cytosolic-free Ca^{2+} was observed in the ventral ectoderm, mesoderm, or endoderm. We also showed that the Ca^{2+} transients require functional L-type voltage-sensitive Ca^{2+} channels, as treatment with the specific channel antagonist R(+) BayK 8644 led to their complete inhibition during gastrulation. In addition, R(+)BayK 8644 led to a reduction in the expression of the early neuralizing genes *Zic3* and *geminin*, and resulted in severe defects in the subsequent formation of the anterior nervous system (Leclerc et al., 2000).

Here, we further explore the relationship between the Ca^{2+} transients observed and the expression of early neural genes. However, studying the interaction between Ca^{2+} signaling and gene expression during neural induction in intact embryos is complicated by the fact that (1) The whole embryo is a three-dimensional structure where the dorsal ectoderm receives both planar and vertical signals from the mesoderm. Planar signals are those that are able to travel from the anterior mesoderm to the posterior ectoderm, while vertical signals occur when the mesoderm has involuted into the interior of the embryo and so signals can also pass from the underlying mesoderm to the overlying ectoderm during the later stages of gastrulation. (2) In the whole embryo, during gastrulation, not only the mesoderm undergoes convergent extension movements. (3) The deep of field given by the 5× objective used to record Ca^{2+} transients in the whole embryo does not allow to have a complete view of the dorsal ectoderm. Thus, in an attempt to simplify the experimental model and to correlate Ca^{2+} pattern with the expression pattern of early neural gene, we used Keller open-face explants (Keller and Danilchik, 1988) as a two-dimensional system to study neural induction. In such explants, convergence and extension movements only occur in the mesoderm but not in the ectoderm (Keller et al., 1992). The explant extends from the bottle cells on the blastopore lip up toward the animal pole. In order to eliminate vertical contact with the prospective neuroectoderm, open-faced explants are made at initial gastrula stage (i.e., at stage 10, 9 h postfertilization; hpf) and are maintained flat under a coverslip. At this stage, the blastoporal groove is not yet formed, therefore mesodermal involution has not occurred (Nieuwkoop and Faber, 1967). Extensive experiments by Keller et al., (1992) have established that this type of assay eliminates vertical interactions between mesoderm and ectoderm. Thus, in these explants, only planar signals pass from the mesoderm to the ectoderm. These signals have been shown to be sufficient to reproduce many aspects of neural induction observed in vivo, such as the expression of neural marker genes, neuronal differentiation, and the induction of a regionalized neural plate along the anteroposterior axis (Doniach, 1992).

Again using aequorin and a PIM, we have imaged the Ca^{2+} dynamics during neural induction in Keller open-face explants. A series of Ca^{2+} transients were observed in groups of ectoderm cells. As in intact embryos, these transients resulted from the activation of L-type Ca^{2+} channels. In addition, while the pattern of individual ectodermal Ca^{2+} transients appeared to be random with respect to both location and timing, the accumulated pattern correlated with the expression of the early neural precursor gene, *Zic3*. Furthermore, when the transients were blocked with the L-type Ca^{2+} channel antagonist, nifedipine, the level of *Zic3* expression was dramatically reduced. We conclude that in open-face explants, planar signals reproduce Ca^{2+} -signaling patterns observed in the dorsal ectoderm of intact embryos and that the accumulated effect of the localized Ca^{2+} transients over time may play a role in controlling the expression of the early neural gene, *Zic3*.

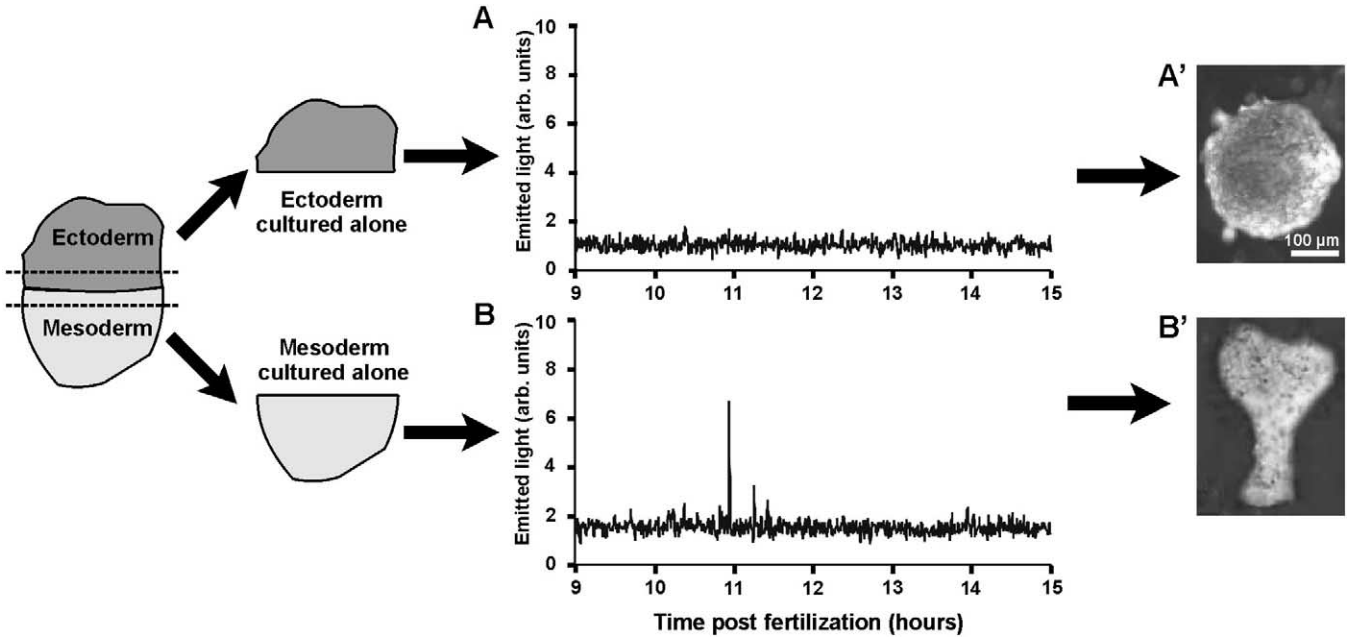

Fig. 2. Isolated culture of separated ectoderm and mesoderm portions of the explant. (A, B) Representative temporal traces obtained for the separated ectoderm and mesoderm portions. No signal was recorded from the isolated ectoderm (A), whereas a few signals were recorded from the isolated mesoderm (B). (A′, B′) At the end of the experiment, the ectoderm differentiated into a constricted ball of tissue (A′), while the mesoderm underwent convergence and extension to form an elongated structure (B′).

Materials and methods

Embryos and explant preparation

Eggs were obtained from female *Xenopus* that had been primed 12–15 h earlier with 500 U of Human Chorionic Gonadotrophin (Organon, Holland). Oocytes were fertilized in vitro with macerated testis and then dejellied with 2% cysteine, pH 8.0, after which they were incubated at room temperature (~22°C) in 0.1× Normal Amphibian Medium (NAM: 110 mM NaCl, 2 mM KCl, 1 mM $NaHCO_3$, 1 mM $MgSO_4$, 1 mM $CaCl_2$, 0.1 mM Na_2EDTA, 1.6 mM Na_2HPO4, 0.4 mM NaH_2PO_4). Staging was performed according to Nieuwkoop and Faber (1967). Open-face explants, consisting of part of the animal cap, the noninvoluting marginal zone (NIMZ), both of which are ectoderm, and the involuting marginal zone (IMZ), which is mesoderm, were dissected at stage 10 (9 hpf) as described by Keller and Danilchick (1988). Head mesoderm, which is composed of loose potentially migratory cells, was removed with a fine platinum wire. Explants were then placed under a piece of coverslip to prevent involution of the mesoderm and cultured in 0.5× NAM with 50μg/ml gentamycin. Open-faced explants undergo convergent extension only in the mesoderm, and only explants that showed symmetrical convergent extension were kept for analysis. In some experiments, the open-face explant was dissected further to give separate ectodermal and mesodermal pieces of tissue.

Microinjection of aequorin

The microinjection pipettes, the pressure injection system, and the other protocols used for injecting *Xenopus* embryos with aequorin are described in detail elsewhere (Webb et al., 1997). Embryos were injected at the two-cell stage with approximately 4 nl of recombinant *f*-aequorin (0.5% in 100 mM KCL, 5 mM Mops, and 50 μM EDTA; Shimomura et al., 1990) into each cell. Embryos were bathed in 0.1× NAM containing 4% Ficoll (Sigma) during injection and for 30 min after the injection. They were then transferred to, and maintained in, 0.1× NAM alone.

Data acquisition, review, and analysis

Temporal aequorin-generated data were collected by a photomultiplier tube (PMT) system, which is described in detail in Lee et al. (1999). Background noise is less than 10 photons/s. Data were collected every 1 s over a period of approximately 10 h. Spatial information from aequorin-generated images and bright field images were acquired by using our custom-designed Photon Imaging Microscope (PIM, Science Wares, USA), which is described in detail elsewhere (Webb et al., 1997; Lee et al., 1999). Backgroung noise is 2 10^{-5} photons/s/pixel. Images were collected by using either Zeiss Fluar 10×/0.5 NA or Plan Neofluar 10×/0.3 NA objectives. Burn-out experiments using Triton X-100 to lyse the explant showed that when signals were not observed (i.e., such as when the ectoderm explants were

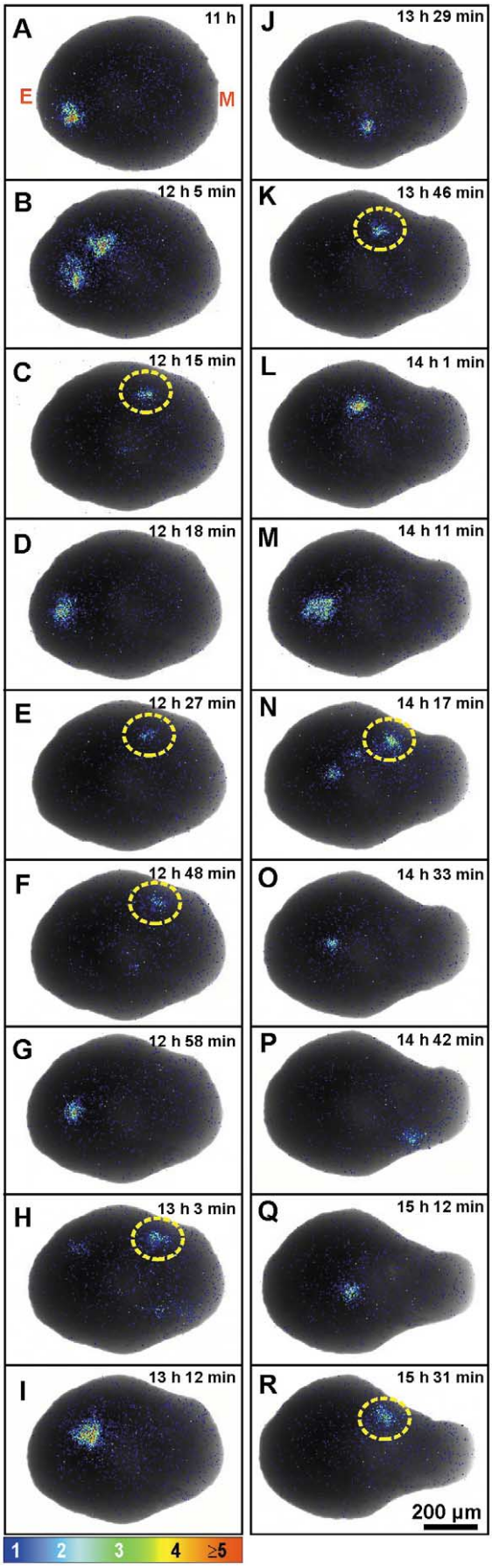

cultured alone or when explants were incubated in 300 μM nifedipine), aequorin was not a limiting factor.

At the end of data acquisition, files were downloaded into Corel DRAW 8 and PHOTO PAINT 8 (Corel Corp., USA) for figure preparation and presentation. For subsequent detailed quantitative data analysis, series of photon and corresponding bright-field images were exported in TIFF file format to Metamorph 3.0 (Universal Imaging, Inc., West Chester, PA, USA). In addition, using Simple PCI (Compix, USA), pseudo-3D representations of the cumulative Ca^{2+} level in an explant, over the course of an experiment, were generated. The number of photons was integrated for the complete period of data acquisition (about 6–8 h) and a 3D contour graph was then produced by plotting the total number of photons at each *x*, *y* coordinate on the 2D image of the explant. The figures were then smoothed by using a Gaussian filter feature in Simple PCI. To further enhance the 3D representation, the intensity was coded with a look up table (lut) using a gray scale.

Explants were selected for detailed analysis according to the following criteria: (1) they had not dissociated during the course of the experiment but had clearly elongated; (2) intact control embryos developed normally; and (3) from the background level of luminescence acquired, aequorin-loading was deemed to be successful.

Ca^{2+} transients are known to arise in response to mechanical stimulation or wounding in many systems (Sanderson et al., 1994). Such injury signals were observed from the explants on several occasions, especially at the start of an experiment and especially at the periphery of the explant. These signals died down within a few minutes after imaging had started. However, during the course of an experiment, cells were sometimes seen to bleb off the edges of an explant, and so generate confusing signals. Thus, in the analysis protocols, we only used the center portions of the ectoderm and mesoderm for a comparative analysis so as to avoid possible signaling artifacts generated by explant edges.

Incubation with Nifedipine and BAPTA-AM

Aequorin-loaded embryos were incubated in the dark with the L-type Ca^{2+} channel antagonist nifedipine (Sigma) or with the Ca^{2+} buffer BAPTA-AM (Molecular Probes) for 30 min prior to explant preparation, after which the explants were incubated with nifedipine or BAPTA-AM for the duration of data acquisition. Nifedipine and BAPTA-AM were prepared as 50 and 4 mM

Fig. 3. Representative example of the Ca^{2+} signaling events observed in an explant for approximately 4.5 h starting at 11 hpf (A). Each panel represents 120 s of accumulated light. The area circled in yellow in (C, E, F, H, K, N, and R) highlights a repetitive signal at the dorsal ectoderm–mesoderm border. Color scale indicates luminescent flux in photons/pixel. E and M are ectoderm and mesoderm, respectively.

stock solutions, respectively, in dimethyl sulfoxide (DMSO) and diluted to either 150 or 300 μM (nifedipine) and 0.4 μM (BAPTA-AM) in 0.1× NAM just prior to use.

In situ hybridization

In situ hybridization was performed on the open-face explants as described by Harland (1991) using a fluorescein-labeled antisense probe for *Xenopus Zic3* (Nakata et al., 1997).

Results

Temporal traces of Ca^{2+} signaling from open-face explants

Fig. 1A shows a representative trace ($n = 5$) obtained from an aequorin-loaded explant using a PMT. Two components were reported: (1) A slow-rising component, i.e., a gradual increase in the level of Ca^{2+} that reached a maximum at around 10 hpf (stage 10.25 for sibling whole embryos). Since previous studies performed on whole embryos indicate that the onset of Ca^{2+} transients occurs at stage 8–9 (Leclerc et al., 2000), this slow-rising component is probably well underway at the start of the measurement. (2) Superimposed on this gradual change in Ca^{2+} concentration was a series of rapid Ca^{2+} transients that started at around 10.5 hpf and that appeared as vertical spikes on the time scale used. The average number of Ca^{2+} transients from these five explants was also calculated over time (see Fig. 1B). The number of events increased from 9.2 ± 2.7 at stage 10 to a maximum of 20.6 ± 2.4 at stage 11 and then decreased to 17.5 ± 2.7 and 11.9 ± 3.5 at stages 12 and 13, respectively.

Ca^{2+} transients from separated ectoderm and mesoderm

Open-face explants were prepared as usual and then were divided further to give three separate pieces of tissue: ectoderm, mesoderm, and the ectoderm/mesoderm border. The border was discarded, and the mesoderm and ectoderm were cultured in separate dishes. The ectoderm explant ($n = 5$) showed no Ca^{2+} signals throughout the entire period it was imaged (Fig. 2A), whereas the mesoderm explant ($n = 5$) produced a few Ca^{2+} spikes (Fig. 2B). Furthermore, the ectoderm portion constricted to form a ball, characteristic of the atypical epidermis that forms when ectoderm is not induced to follow a neural pathway (Fig. 2A′), while the mesoderm portion converged and extended, as it would have done in an intact explant (Fig. 2B′).

Spatial characteristics of the Ca^{2+} transients

In order to further explore the role played by Ca^{2+} during neural induction, a detailed analysis was performed in an attempt to search for spatial patterns of explant-generated transients that might shed some light on their possible developmental function. Fifteen different open-faced explants were analyzed by using the imaging data acquired with our PIM. As illustrated by photon counting images of a representative open-faced explant, the individual signaling events seemed to be random with respect to time and location within the explant (Fig. 3). Certain groups of cells were observed to signal several times during the course of the experiment. The location of such repetitive signaling domains varied with some from the ectoderm, others from the mesoderm, and some from the ectoderm/mesoderm border. A representative example of such a repetitive signaling domain (highlighted in yellow) on the ectoderm/mesoderm border is shown in Fig. 3.

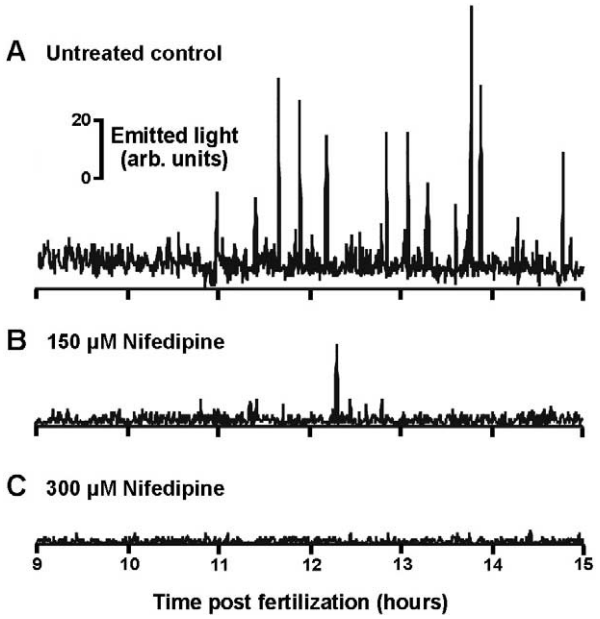

Fig. 4. The effect of nifedipine on Ca^{2+} transients. Three representative temporal traces from aequorin-loaded explants that were (A) maintained under normal conditions (control) or treated with either (B) 150 μM nifedipine or (C) 300 μM nifedipine. Nifedipine suppresses the Ca^{2+} transients in a dose-dependent manner at 150 μM, both the amplitude and the number of transients are reduced when compared with the untreated controls, and at 300 μM all of the transients are completely inhibited.

Nifedipine suppresses Ca^{2+} transients in a dose-dependent manner

A specific L-type Ca^{2+} channel (LTC) antagonist, nifedipine, was used to determine whether the Ca^{2+} signaling events observed in the explants were due to an influx of extracellular Ca^{2+} via voltage-gated channels. The effect of nifedipine appears to be dose-dependent (Fig. 4; $n = 4$ for all experiments): at 150 μM (Fig. 4B), both the number and amplitude of Ca^{2+} spikes were noticeably decreased when compared with the untreated control explants (Fig. 4A), while at 300 μM, all of the spikes were completely inhibited

(Fig. 4C). In order to confirm that the lack of signal observed in the 300 μM nifedipine-treated explants was due to the antagonist rather than being limited by the amount of aequorin loaded into explants, they were incubated with 1% Triton X-100 in 0.1× NAM at the end of each experiment to "burn-out" the remaining unspent aequorin (data not shown).

Correlation of localized non-propagating Ca^{2+} transients and early neural gene expression

In order to analyze the relation between patterns of Ca^{2+} transients and neural determination, we have followed the expression of *Zic3* in open-faced explants. *Zic3* is one of the earliest neuralizing gene that is positively regulated by chordin and that can induce the expression of other proneural genes, such as *XIPOU2* and *neurogenin* (Nakata et al., 1997). The pattern of *Zic3* expression in open-faced explants at a stage corresponding to stage 12.5–13 in sibling embryos was examined by using whole-mount in situ hybridization. Here, we showed for the first time that this pattern is detected as a crescent in the posterior-most region of the ectoderm and appeared to be very reproducible in all open-faced explants observed ($n = 50$). Fig. 5 gives representative examples of such pattern for four different open-faced explants.

An accumulation of all the individual localized non-propagating Ca^{2+} transients was plotted on an outline of each converging and elongating explant over the course of gastrulation. These are shown in Fig. 6Aii. This clearly illustrates the fact that certain domains of the explant do not signal at all, whereas others are responsible for generating most of the signal. In general, the ectoderm/mesoderm border and the NIMZ of the ectoderm appear to generate most signal during gastrulation. When these same explants were then fixed at a stage corresponding to stage 12 in intact embryos, *Zic3* expression was detected as a crescent in the posterior-most region of the ectoderm (Fig. 6Ai), overlapping the accumulated Ca^{2+} increase ($n = 5$). To determine whether these initial Ca^{2+} signals could be sufficient to support *Zic3* expression, aequorin-loaded Keller explants were incubated with BAPTA-AM (0.4 μM) for 8 h during gastrulation. In BAPTA-treated explants ($n = 3$), no significant Ca^{2+} increase was observed and the expression of *Zic3* was dramatically reduced (Fig. 6B). Additional control experiments to confirm the effect of the inhibition of intracellular Ca^{2+} increase on *Zic3* expression were performed with open-faced explants which were not loaded with aequorin. Fig. 6C compares the level of *Zic3* expression in two representative groups of control and BAPTA-treated open-faced explants which have been processed simultaneously for whole-mount in situ hybridization ($n = 38$). Altogether, these data indicate that an inhibition of Ca^{2+} in Keller explants can disrupt the expression of transcription factors involved in neural induction.

Discussion

Temporal traces of Ca^{2+} signaling from intact embryos and explants show similar components

Excluding mesoderm involution, the cellular events observed in the explants are known to be representative of the morphogenetic events that occur in intact embryos during this period of development (Keller and Danilchik, 1988). In addition to the morphological similarities between intact embryos and open-face explants, we show that temporal similarities in Ca^{2+} signaling profiles also occur during gastrulation. We have previously presented the data obtained from an aequorin-injected intact embryo by using a PMT (Fig. 1A in Leclerc et al., 2000). Two components were reported: (1) A slow-rising component, i.e., a gradual increase in the level of Ca^{2+} starting just after 5 hpf (stage 8), which reached a maximum at about 9 hpf (stage 10) and then returned to its original resting value by approximately 15 hpf (stage 13). (2) Superimposed on this gradual change in Ca^{2+} concentration was a series of rapid Ca^{2+} transients, which appeared as vertical spikes on the time scale used. Both of these components were also present in the PMT traces recorded from explants (see Fig. 1). As open-faced explants cannot be made until the blastopore lip is visible, i.e., 9 hpf (stage 10), it is clear that the slow rise should be well underway by this time. What is seen, therefore, in the case of the explant trace could possibly be the latter stages of the slow rise, delayed somewhat by the stress of explant excision. Thus, in the case of the explant, the rapid spiking does not occur in earnest until around 10.5 hpf (stage 10.25) compared with 8.5 hpf in intact embryos (stage 9+).

Comparison of the numerical profile of Ca^{2+} events between intact embryos and explants during gastrulation

A comparison of the average number of Ca^{2+} transients from explants with those from intact embryos (Fig. 4D in Leclerc et al., 2000) indicates that the overall profile of events is the same with respect to their developmental stages, i.e., the number rises to a maximum number of events occurring at stage 11 in both cases then falls through stages 12 to 13. However, in general, the number of events appears to be approximately four times higher for intact embryos than in explants. This may however be partly due to the fact that only a portion of the dorsal ectoderm was removed when making the explant, leading to a smaller surface area of the presumptive neural plate being examined. Thus, with regards to the rapid spiking events, explants also seem to behave in a manner similar to intact embryos.

Groups of cells (between 4 and 20) appeared to signal near-simultaneously, and there was no propagation of the Ca^{2+} signal beyond the spatial boundaries of the initial transient. These signals were thus designated as being "localized nonpropagating Ca^{2+} transients." They appear,

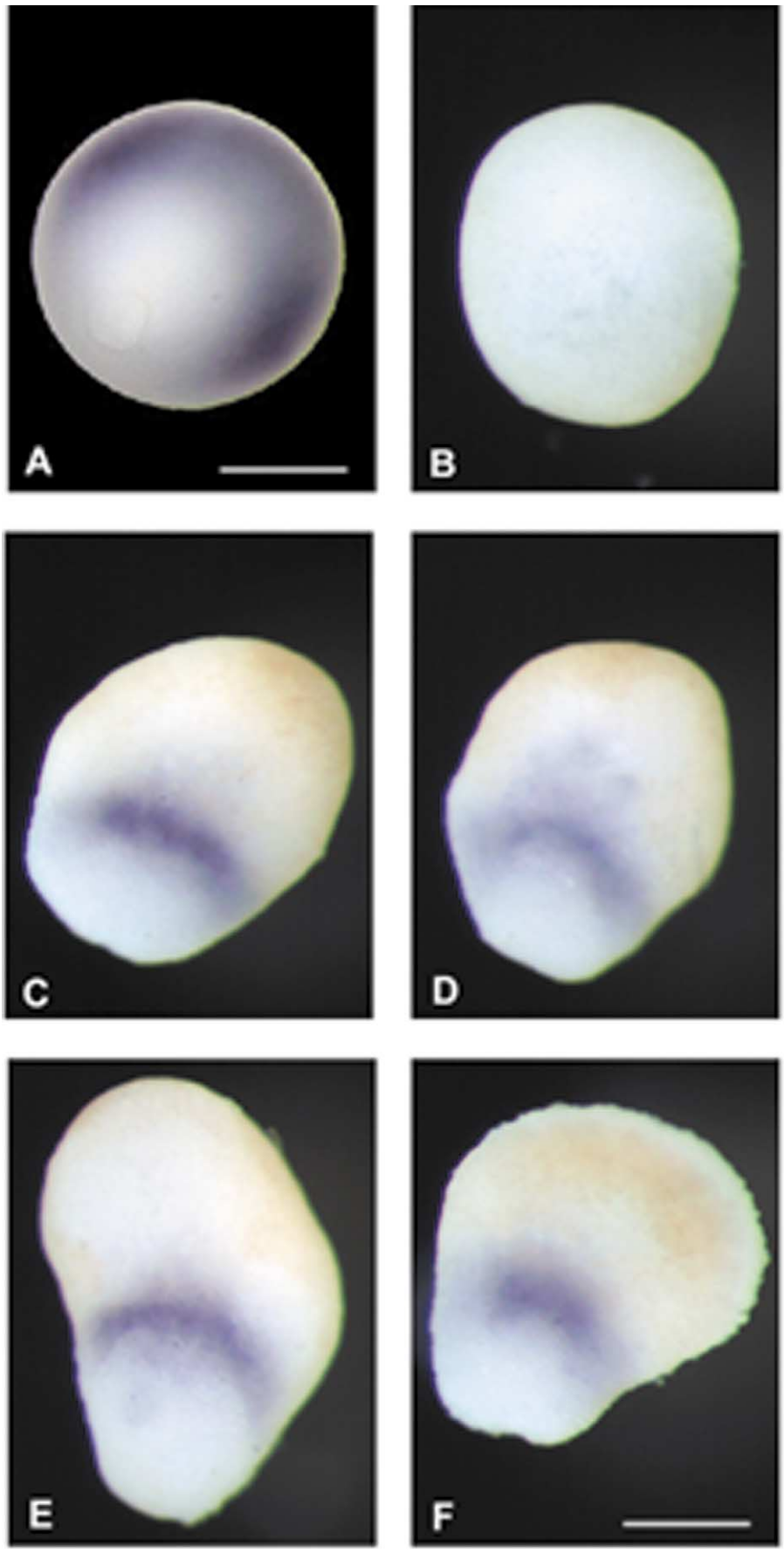

Fig. 5. Detection of Zic3 by whole-mount in situ hybridization in whole control embryo and in explants. (A) Zic3 expression in stage 12 control embryo; dorsal view, anterior up. (B) Isolated dorsal ectoderm (sibling control embryos at stage 12). (C–F) Four different open-faced explants showing the crescent shape staining in the posterior-most region of the ectoderm; dorsal view, animal pole up. Scales bars in (A) 500 μm, in (B–F) 200 μm.

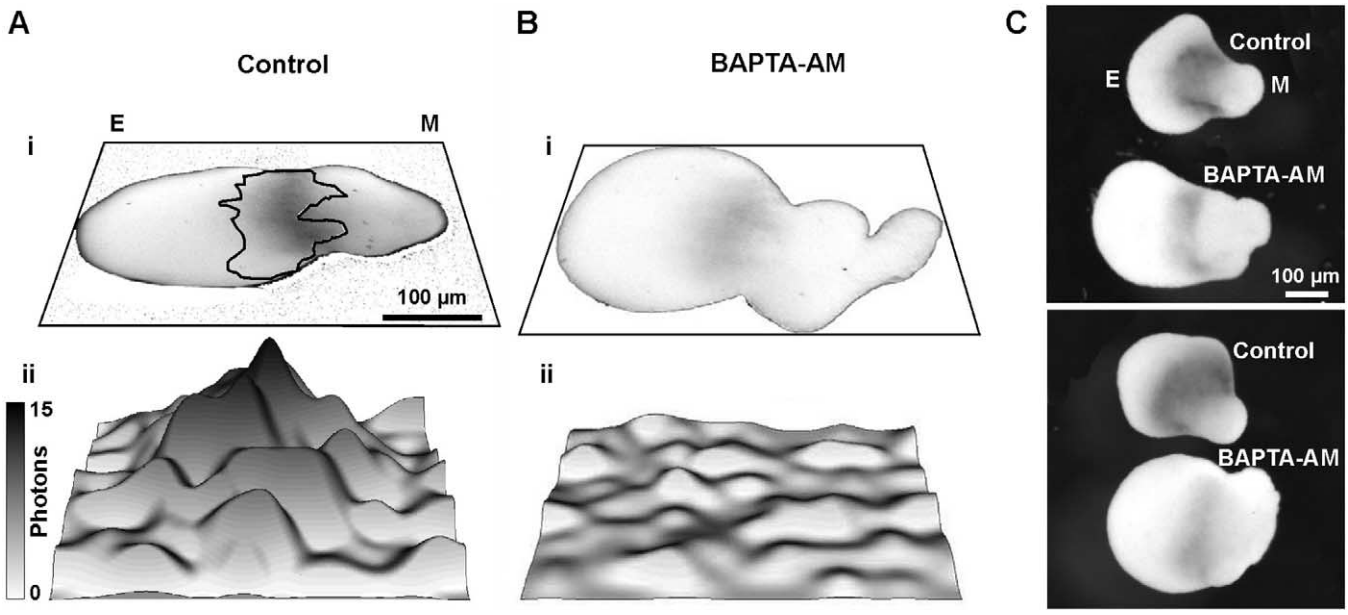

Fig. 6. Comparison of the expression of *Zic3* with the accumulated location of Ca^{2+} transients. Representative aequorin-loaded ($n = 5$) (A) untreated control and (B) BAPTA-AM treated explants to show (ii) pseudo-3D profile of accumulated increase in $[Ca^{2+}]_i$ during the 8 h of data acquisition that corresponds to gastrulation and (i) the subsequent expression pattern of *Zic3*, determined by *in situ* hybridization in the same explant. The Ca^{2+} increase above the background (5 photons) is outlined in black in (Ai) to show that this region correlates with the pattern of *Zic3* expression. (C) Representative examples of untreated control and BAPTA-AM-treated explants to show Zic3 expression ($n = 38$, 4 independent experiments). E and M are ectoderm and mesoderm, respectively.

therefore, to be similar to the localized nonpropagating Ca^{2+} transients observed in the anterior dorsal ectoderm in intact embryos before the mid-gastrula stage (stage 11.5; Leclerc et al., 2000). No intercellular propagating Ca^{2+} waves were detected from any explant throughout the course of an experiment (i.e., up to ~stage 13, 15 hpf) as seen in intact embryos during the same period (Leclerc et al., 2000).

In amphibian, in addition to its role during meiosis (Wasserman and Masui, 1975; Moreau et al., 1980) and fertilization (Busa and Nuccitelli, 1985), calcium has been shown to be involved in convergent extension movements at gastrulation, dorsoventral patterning of the mesoderm (Kume et al., 2000a, b), and neural determination. Recent data strongly suggest that morphogenetic movements at gastrulation are regulated by the Wnt/Ca^{2+} signaling pathway (Wallingford et al., 2001a; Choi and Han, 2002). Indeed, Ca^{2+} transients have been described by Wallingford et al. (2001b), who showed that they arised stochastically and demonstrated that they play a direct role in coordinating convergent extension cell movements during mesoderm elongation, and are independent of neural induction. We also observed Ca^{2+} transients in the mesoderm region of the explant, but with a lower frequency and intensity than those recorded in the ectoderm. In *Xenopus*, many lines of evidence have implicated an increase in intracellular calcium ($[Ca^{2+}]_i$) as a sufficient signal that directly leads to neural determination. Neuralization can be obtained by dissociation of animal caps in calcium free medium. In earlier experiments, we found that the dissociation triggers an increase in $[Ca^{2+}]_i$. When ectodermal cells are loaded with the calcium chelator BAPTA, the neuralization was blocked, the neural marker NCAM is not expressed (Leclerc et al., 2001). In animal caps, neuralization can also be obtained by direct stimulation of dihydropyridine-sensitive Ca^{2+} channels with dihydropyridine agonist or of intracellular calcium stores with caffeine; this leads to *XIPOU2* expression in 30 min and *NCAM* expression after 3 h (unpublished results). Other evidences have shown that direct activation of dihydropyridine-sensitive Ca^{2+} channels is able to convert ectoderm into neuroectoderm (Moreau et al., 1994; Leclerc et al., 1997). It should be noticed that overexpression of the heterologous α_{1C} subunit of the dihydropyridine-sensitive Ca^{2+} channels in animal caps failed to induce the neural-marker *Xsox-2* (Palma et al., 2001). However, while *Zic3* and *XIPOU2* are sufficient to direct ectoderm cells to neural fate (Nakata et al., 1997; Witta et al., 1995), *Xsox-2* alone is not (Mizuseki et al., 1998). Thus, it is possible that *Xsox-2*, which does not display an instructive role in early neural development (Kishi et al., 2000), is regulated via a mechanism different from the one of *Zic3*, independent of Ca^{2+} signals.

What might be the target(s) of the $[Ca^{2+}]_i$ increase seen in the ectoderm? We have previously shown that, in the whole embryo, Ca^{2+} is necessary and sufficient to trigger neural induction (Moreau et al., 1994) and necessary to activate transcription factors, such as *Zic3* or *geminin*, involved in neural induction (Leclerc et al., 2000). Ca^{2+}

transients were only observed in the anterior part of the dorsal ectoderm, where the anterior neural structures form. However, it is difficult to correlate Ca^{2+} transients and gene expression in the whole embryo (Leclerc et al., 2000). Here, using Keller explants, we show that planar signals coming from the mesoderm are sufficient to trigger an increase in intracellular in Ca^{2+} in distinct parts of the ectoderm. When examined with a short integration time, these signals seem to occur stochastically throughout this region. However, when we accumulate Ca^{2+} transients during the entire recording period, it is clear that they are restricted to a localized area in the posterior ectoderm. Whole-mount in situ hybridization of these same explants indicates that *Zic3* expression is also localized in this area. Although BAPTA-AM produces a complete inhibition of the Ca^{2+} increase, the level of *Zic3* expression is not abolished totally. These observations may be due to several factors. BAPTA-AM permeates freely into cells; however, this ester derivative needs to be deesterified in order to chelate calcium. The rate at which this form accumulates into the cytosol in the fully deesterified form is affected by the temperature and the pH of the medium. Under our conditions, we estimate that 30 min is a sufficient time. However, it is not possible to precisely control the concentration of chelator loaded in the explants. Since open-faced explants were prepared at stage 10; about 2 h after the onset of Ca^{2+} transients in the whole embryos (Leclerc et al., 1997; 2000), this delay (2.5 h) may be sufficient to explain the low level of *Zic3* expression observed in BAPTA-treated explants. It should also be consider that Ca^{2+} imaging starts immediately after BAPTA treatment. On the one hand, it is possible that Ca^{2+} transients in BAPTA-loaded explants are below the background level of the detection system (5 photons). As the neural gene *Zic3* is expressed in a portion of the Ca^{2+} transients area, we thus propose a direct correlation between the pattern of Ca^{2+} transients and at least one transcription factor (Zic 3) controlling neural determination. However, one cannot excluded that the expression of *Zic3* may be controlled by a Ca^{2+}-dependent and a Ca^{2+} independent mechanism. The random nature of the Ca^{2+} transients with respect to time and space may relate to the dynamic nature of the entry channels involved (i.e., the L-type Ca^{2+} channels) which may not be expressed or activated everywhere in the ectoderm at the same time. We have previously shown that Ca^{2+} channels, which reflect neural competence (Drean et al., 1995; Leclerc et al., 1995), are expressed transiently, gradually, and independently in separate groups of ectodermal cells during gastrulation.

What might be the nature of the signal that activates the Ca^{2+} channels? L-type Ca^{2+} channels are voltage-dependant and therefore need a depolarization of the plasma membrane to open. Thus, during neural determination, this suggests a link between noggin/BMP signaling and the activation of L-type Ca^{2+} channels. We propose that this link may be represented by FGF receptors. It has been shown by Launay et al. (1997) that the integrity of FGF receptors is necessary to allow noggin to act. It is also known that FGF receptors can control either nonspecific cationic channels which can depolarize the membrane (Munaron et al. 1997; Distasi et al., 1998) or L-type Ca^{2+} channels directly (Rosenthal et al., 2001). Work is now in progress to attempt to establish a link between Ca^{2+} channel activation and BMP/noggin signaling. Linking the role of Ca^{2+} channel activity to FGF receptor signaling pathways may further our understanding of the role played by Ca^{2+} in neural determination.

Acknowledgments

We thank Drs. O. Shimomura, Y. Kishi, and S. Inouye for supplying us with *f*-aequorin and Dr. J. Aruga for providing the *Xenopus Zic3* DNA and Christiane Daguzan for technical help. This work was supported by a grant from the PROCORE France/Hong Kong Joint Research Scheme sponsored by the Research Grants Council of Hong Kong and the Consulate General of France in Hong Kong (F-HK98/99.SC06) awarded to M.M., A.L.M., C.L., and S.E.W.; a joint PICS grant funded by the Centre National de la Recherche Scientifique (CNRS) and HKUST to M.M., C.L., A.L.M., and S.E.W.; a HK Research Grants Council Grant HKUST6106/01M awarded to A.L.M and S.E.W.; and an Association pour la Recherche sur le Cancer (ARC) grant awarded to M.M.

References

Busa, W.B., Nuccitelli, R., 1985. An elevated free cytosolic Ca^{2+} wave follows fertilization in eggs of the frog, *Xenopus laevis*. J. Cell Biol. 100, 1325–1329.

Choi, S.C., Han, J.K., 2002. Xenopus Cdc42 regulates convergent extension movements during gastrulation through Wnt/Ca^{2+} signaling pathway. Dev. Biol. 244, 342–357.

Distasi, C., Torre, M., Antoniotti, S., Munaron, L., Lovisolo, D., 1998. Neuronal survival and calcium influx induced by basic fibroblast growth factor in chick ciliary ganglion neurons. Eur. J. Neurosci. 10, 2276–2286.

Doniach, T., 1992. Induction of anteroposterior neural pattern in Xenopus by planar signals. Dev. Suppl., 183–193.

Drean, G., Leclerc, C., Duprat, A.M., Moreau, M., 1995. Expression of L-type Ca^{2+} channel during early embryogenesis in *Xenopus laevis*. Int. J. Dev. Biol. 39, 1027–1032.

Hamburger, V., 1988. The Heritage of Experimental Embryology: Hans Spemann and the Organizer. Oxford University Press, Oxford.

Harland, R.M., 1991. In situ hybridization: an improved whole-mount method for Xenopus embryos. Methods Cell Biol. 36, 685–695.

Hawley, S.H., Wunnenberg-Stapleton, K., Hashimoto, C., Laurent, M.N., Watabe, T., Blumberg, B.W., Cho, K.W., 1995. Disruption of BMP signals in embryonic Xenopus ectoderm leads to direct neural induction. Genes Dev. 9, 2923–2935.

Hemmati-Brivanlou, A., Kelly, O.G., Melton, D.A., 1994. Follistatin, an antagonist of activin, is expressed in the Spemann organizer and displays direct neuralizing activity. Cell 77, 283–295.

Keller, R., Danilchik, M., 1988. Regional expression, pattern and timing of convergence and extension during gastrulation of *Xenopus laevis*. Development 103, 193–209.

Keller, R., Shih, J., Sater, A.K., Moreno, C., 1992. Planar induction of convergence and extension of the neural plate by the organizer of Xenopus. Dev. Dyn. 193, 218–234.

Kishi, M., Mizuseki, K., Sasai, N., Yamazaki, H., Shiota, K., Nakanishi, S., Sasai, Y., 2000. Requirement of Sox2-mediated signaling for differentiation of early Xenopus neuroectoderm. Development 127, 791–800.

Kume, S., Inoue, T., Mikoshiba, K., 2000a. Galphas family G proteins activate IP(3)-Ca(2+) signaling via gbetagamma and transduce ventralizing signals in Xenopus. Dev. Biol. 226, 88–103.

Kume, S., Saneyoshi, T., Mikoshiba, K., 2000b. Desensitization of IP3-induced Ca^{2+} release by overexpression of a constitutively active Gqalpha protein converts ventral to dorsal fate in Xenopus early embryos. Dev. Growth Differ. 42, 327–335.

Lamb, T.M., Knecht, A.K., Smith, W.C., Stachel, S.E., Economides, A.N., Stahl, N., Yancopolous, G.D., Harland, R.M., 1993. Neural induction by the secreted polypeptide noggin. Science 262, 713–718.

Launay, C., Fromentoux, V., Shi, D.L., Boucaut, J.C., 1996. A truncated FGF receptor blocks neural induction by endogenous Xenopus inducers. Development 122, 869–880.

Leclerc, C., Daguzan, C., Nicolas, M.T., Chabret, C., Duprat, A.M., Moreau, M., 1997. L-type calcium channel activation controls the in vivo transduction of the neuralizing signal in the amphibian embryos. Mech. Dev. 64, 105–110.

Leclerc, C., Duprat, A.M., Moreau, M., 1995. In vivo labelling of L-type Ca^{2+} channels by fluorescent dihydropyridine: correlation between ontogenesis of the channels and the acquisition of neural competence in ecotderm cells from Pleurodeles waltl embryos. Cell Calcium 17, 216–224.

Leclerc, C., Rizzo, C., Daguzan, C., Neant, I., Batut, J., Auge, B., Moreau, M., 2001. Neural determination in *Xenopus laevis* embryos: control of early neural gene expression by calcium. J. Soc. Biol. 195, 327–337.

Leclerc, C., Webb, S.E., Daguzan, C., Moreau, M., Miller, A.L., 2000. Imaging patterns of calcium transients during neural induction in *Xenopus laevis* embryos. J. Cell Sci. 113, 3519–3529.

Lee, K.W., Webb, S.E., Miller, A.L., 1999. A wave of free cytosolic calcium traverses zebrafish eggs on activation. Dev. Biol. 214, 168–180.

Mizuseki, K., Kishi, M., Matsui, M., Nakanishi, S., Sasai, Y., 1998. Xenopus Zic-related-1 and Sox-2, two factors induced by chordin, have distinct activities in the initiation of neural induction. Development 125, 579–587.

Moreau, M., Leclerc, C., Gualandris-Parisot, L., Duprat, A.-M., 1994. Increased internal Ca^{2+} mediates neural induction in the amphibian embryo. Proc. Natl. Acad. Sci. USA 91, 12639–12643.

Moreau, M., Vilain, J.P., Guerrier, P., 1980. Free calcium changes associated with hormone action in amphibian oocytes. Dev. Biol. 78, 201–214.

Munaron, L., Antoniotti, S., Distasi, C., Lovisolo, D., 1997. Arachidonic acid mediates calcium influx induced by basic fibroblast growth factor in Balb-c 3T3 fibroblasts. Cell Calcium 22, 179–188.

Nakata, K., Nagai, T., Aruga, J., Mikoshiba, K., 1997. *Xenopus Zic3*, a primary regulator both in neural and neural crest development. Proc. Natl. Acad. Sci. USA 94, 11980–11985.

Nieuwkoop, P.D., Faber, J., 1967. Normal Table of *Xenopus laevis* (Daudin). North Holland, Amsterdam.

Palma, V., Kukuljan, M., Mayor, R., 2001. Calcium mediates dorsoventral patterning of mesoderm in Xenopus. Curr. Biol. 11, 1606–1610.

Rosenthal, R., Thieme, H., Strauss, O., 2001. Fibroblast growth factor receptor 2 (FGFR2) in brain neurons and retinal pigment epithelial cells act via stimulation of neuroendocrine L-type channels (Ca(v)1.3). FASEB. 15, 970–977.

Sanderson, M.J., Charles, A.C., Boitano, S., Dirksen, E.R., 1994. Mechanisms and function of intercellular calcium signaling. Mol. Cell. Endocrinol. 98, 173–187.

Sasai, Y., De Robertis, E.M., 1997. Ectodermal patterning in vertebrate embryos. Dev. Biol. 182, 5–20.

Sasai, Y., Lu, B., Steinbeisser, H., De Robertis, E.M., 1995. Regulation of neural induction by the Chd and Bmp-4 antagonistic patterning signals in Xenopus. Nature 377, 757.

Shimomura, O., Inouye, S., Musicki, B., Kishi, Y., 1990. Recombinant aequorin and recombinant semi-synthetic aequorins. Cellular Ca^{2+} ion indicators. Biochem. J. 270, 309–312.

Wallingford, J.B., Ewald, A.J., Harland, R.M., Fraser, S.E., 2001a. Calcium signaling during convergent extension in Xenopus. Curr. Biol. 11, 652–661.

Wallingford, J.B., Harland, R.M., 2001. Xenopus Dishevelled signaling regulates both neural and mesodermal convergent extension: parallel forces elongating the body axis. Development 128, 2581–2592.

Wallingford, J.B., Vogeli, K.M., Harland, R.M., 2001b. Regulation of convergent extension in Xenopus by Wnt5a and Frizzled-8 is independent of the canonical Wnt pathway. Int. J. Dev. Biol. 45, 225–227.

Wasserman, W.J., Masui, Y., 1975. Initiation of meiotic maturation in Xenopus laevis oocytes by the combination of divalent cations and ionophore A23187. J. Exp. Zool. 193, 369–375.

Webb, S.E., Lee, K.W., Karplus, E., Miller, A.L., 1997. Localized calcium transients accompany furrow positioning, propagation, and deepening during the early cleavage period of zebrafish embryos. Dev. Biol. 192, 78–92.

Witta, S.E., Agarwal, V.R., Sato, S.M., 1995. XIPOU 2, a noggin-inducible gene, has direct neuralizing activity. Development 121, 721–730.

Zimmerman, L.B., De Jesus-Escobar, J.M., Harland, R.M., 1996. The Spemann organizer signal noggin binds and inactivates bone morphogenetic protein 4. Cell 86, 599–606.